

Supporting Information

A Universal pH range and Highly-efficient Mo₂C-based Electrocatalyst for the
Hydrogen Evolution Reaction

Jiajia Huang, Jingyi Wang, Ruikuan Xie, Zhihong Tian, Guoliang Chai, Yanwu Zhang,*

Feili Lai, Guanjie He, Chuntai Liu, Tianxi Liu, Paul R. Shearing and Dan J.L. Brett*

Corresponding Author

* Guanjie He (g.he@ucl.ac.uk)

* Zhihong Tian (zhihong.tian@zzu.edu.cn)

1. Experimental Section

Table S1. The preparation parameters of different samples.

Samples [Mo ₂ C-xMn@NC]	(NH ₄) ₆ Mo ₇ O ₂₄ · 4H ₂ O [g]	MnCl ₂ · 4H ₂ O [mg]
0.2%Mn	2.48	4
0.5%Mn	2.48	9
1%Mn	2.48	18

Samples [Mo ₂ C-xFe@NC]	(NH ₄) ₆ Mo ₇ O ₂₄ · 4H ₂ O [g]	Fe ₂ (SO ₄) ₃ [mg] [The content is measured in Fe]
0.2%Fe	2.48	8
0.5%Fe	2.48	19
1%Fe	2.48	38

Samples [Mo ₂ C-xCo@NC]	(NH ₄) ₆ Mo ₇ O ₂₄ · 4H ₂ O [g]	Co(NO ₃) ₂ · 6H ₂ O [mg]
0.2%Co	2.48	8
0.5%Co	2.48	20
1%Co	2.48	40

Samples [Mo ₂ C-xNi@NC]	(NH ₄) ₆ Mo ₇ O ₂₄ · 4H ₂ O [g]	NiSO ₄ · 6H ₂ O [mg]
0.2%Ni	2.48	8
0.5%Ni	2.48	19
1%Ni	2.48	38

Figure S1. XRD patterns of M-doped Mo₂C and undoped Mo₂C, M = Mn (a), Co (b), Ni (c).

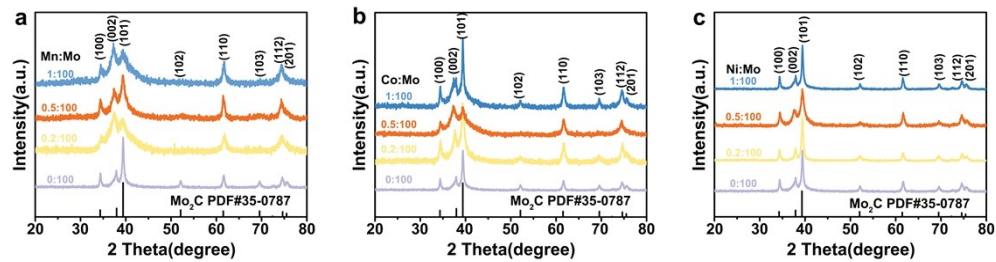


Figure S2. XRD patterns of 0.5%Fe-Mo₂C@NCF and pure Mo₂C zoom-in regions.

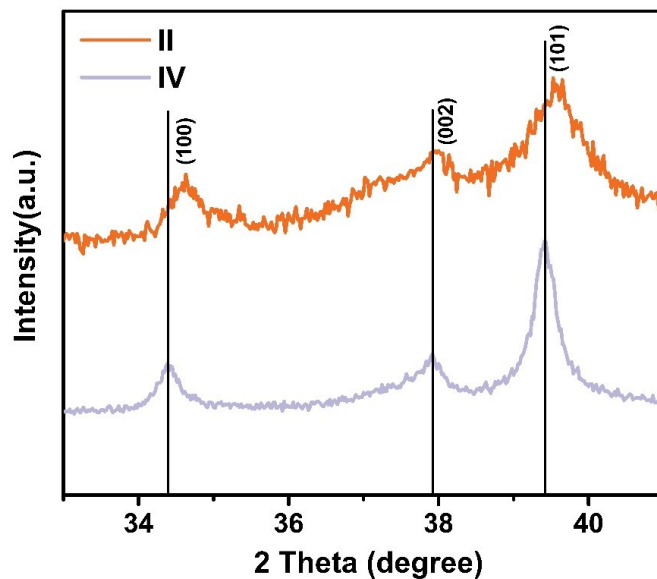


Table S2. Values of lattice parameters, and unit cell volumes for undoped and Fe modified samples.

Catalysts	lattice parameter [Å]		unit cell volume [Å ³]
	a/b	c	
0.2%Fe-Mo ₂ C@NCF	3.0072	4.7490	37.19
0.5%Fe-Mo ₂ C@NCF	3.0068	4.7384	37.10
1%Fe-Mo ₂ C@NCF	3.0060	4.7333	37.04
undoped Mo ₂ C	3.0096	4.7447	37.22

Table S3. Values of BET surface area and TM doping amount of different samples.

Catalysts	Surface area ^{a)} [m ² g ⁻¹]	TM doping amount ^{b)} [wt%]
undoped Mo ₂ C	23.9	0
0.2%Mn-Mo ₂ C@NCF	25.5	0.11% (Mn)
0.5% Mn-Mo ₂ C@NCF	30.7	0.29% (Mn)
1% Mn-Mo ₂ C@NCF	23.4	0.53% (Mn)
0.2%Fe-Mo ₂ C@NCF	27.0	0.21% (Fe)
0.5%Fe-Mo ₂ C@NCF	29.5	0.25% (Fe)
1%Fe-Mo ₂ C@NCF	22.3	0.31% (Fe)
0.2%Co-Mo ₂ C@NCF	23.2	0.14% (Co)
0.5%Co-Mo ₂ C@NCF	28.2	0.22% (Co)
1%Co-Mo ₂ C@NCF	24.7	0.47% (Co)
0.2%Ni-Mo ₂ C@NCF	32.6	0.06% (Ni)
0.5%Ni-Mo ₂ C@NCF	32.1	0.30% (Ni)
1%Ni-Mo ₂ C@NCF	30.1	0.46% (Ni)

a) Based on BET results; b) Data calculated from inductively coupled plasma atomic emission spectroscopy results.

Figure S3. The full XPS profiles of 0.5%Mn-Mo₂C@NCF, 0.5%Fe-Mo₂C@NCF, 0.5%Co-Mo₂C@NCF and 0.5%Ni-Mo₂C@NCF.

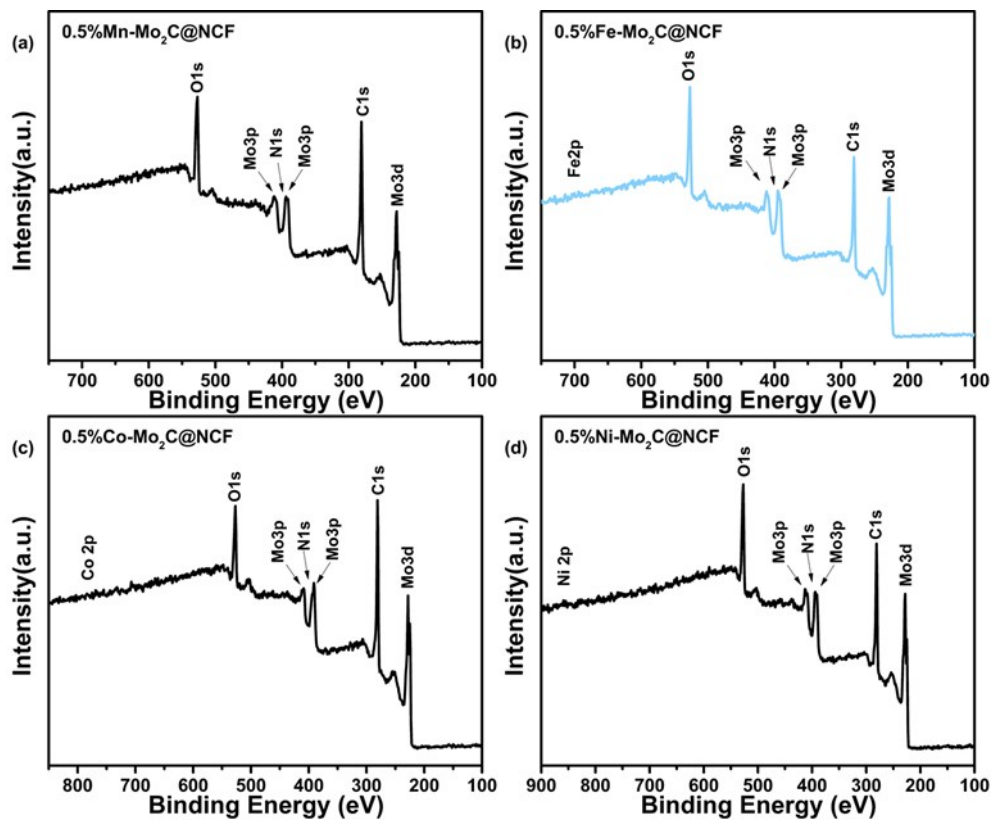


Figure S4. XPS Mo 3d spectra of (a) 0.5%Mn-Mo₂C@NCF, (b) 0.5%Co-Mo₂C@NCF and (c) 0.5%Ni-Mo₂C@NCF, (d) the surface Mo²⁺ percentages of undoped Mo₂C, 0.5%Mn-Mo₂C@NCF, 0.5%Fe-Mo₂C@NCF, 0.5%Co-Mo₂C@NCF and 0.5%Ni-Mo₂C@NCF.

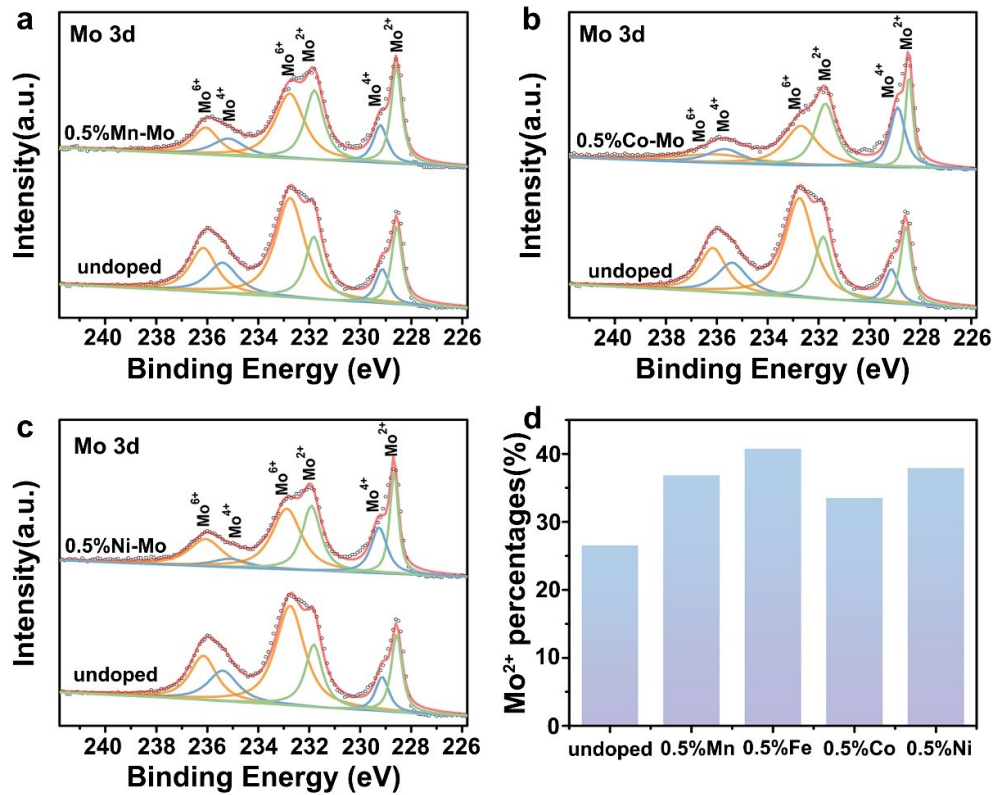


Figure S5. The SEM images of 0.5%Mn-Mo₂C@NCF (a), 0.5%Fe-Mo₂C@NCF (b), 0.5%Co-Mo₂C@NCF (c), 0.5%Ni-Mo₂C@NCF (d).

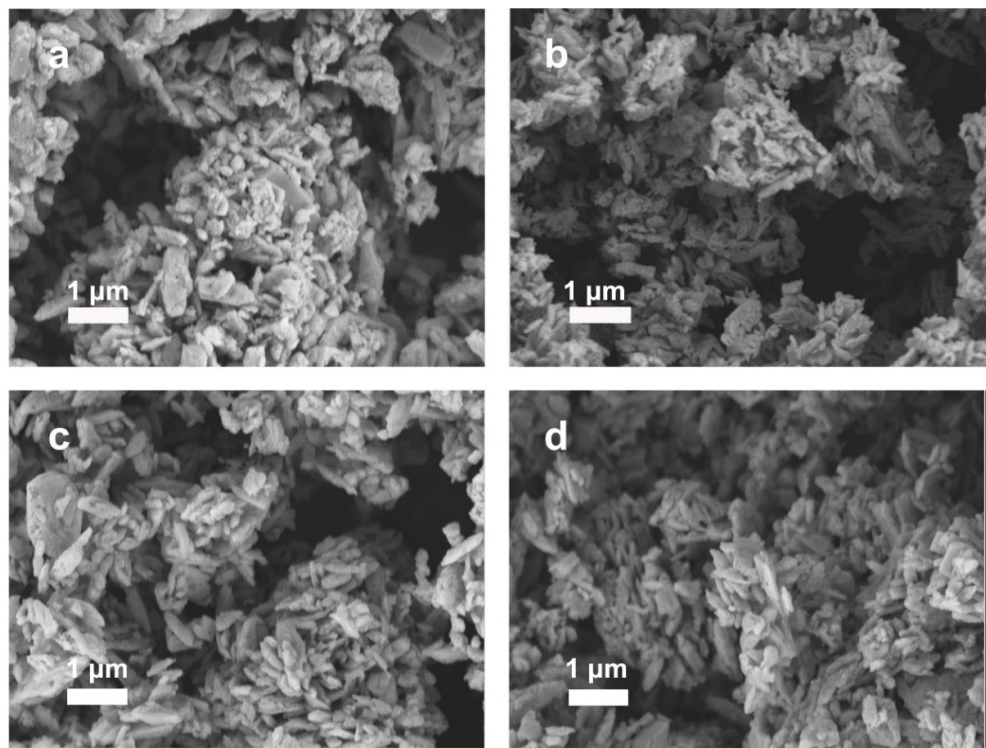


Figure S6. (a) TEM image, (b) HRTEM image, (c) high annular dark-field scanning TEM (HAADF-STEM) images and the corresponding EDS mapping images of 0.5%Mn-Mo₂C@NCF. (d) TEM image, (e) HRTEM image, (f) HAADF-STEM images and the corresponding EDS mapping images of 0.5%Co-Mo₂C@NCF. (g) TEM image, (h) HRTEM image, (i) HAADF-STEM images and the corresponding EDS mapping images of 0.5%Co-Mo₂C@NCF.

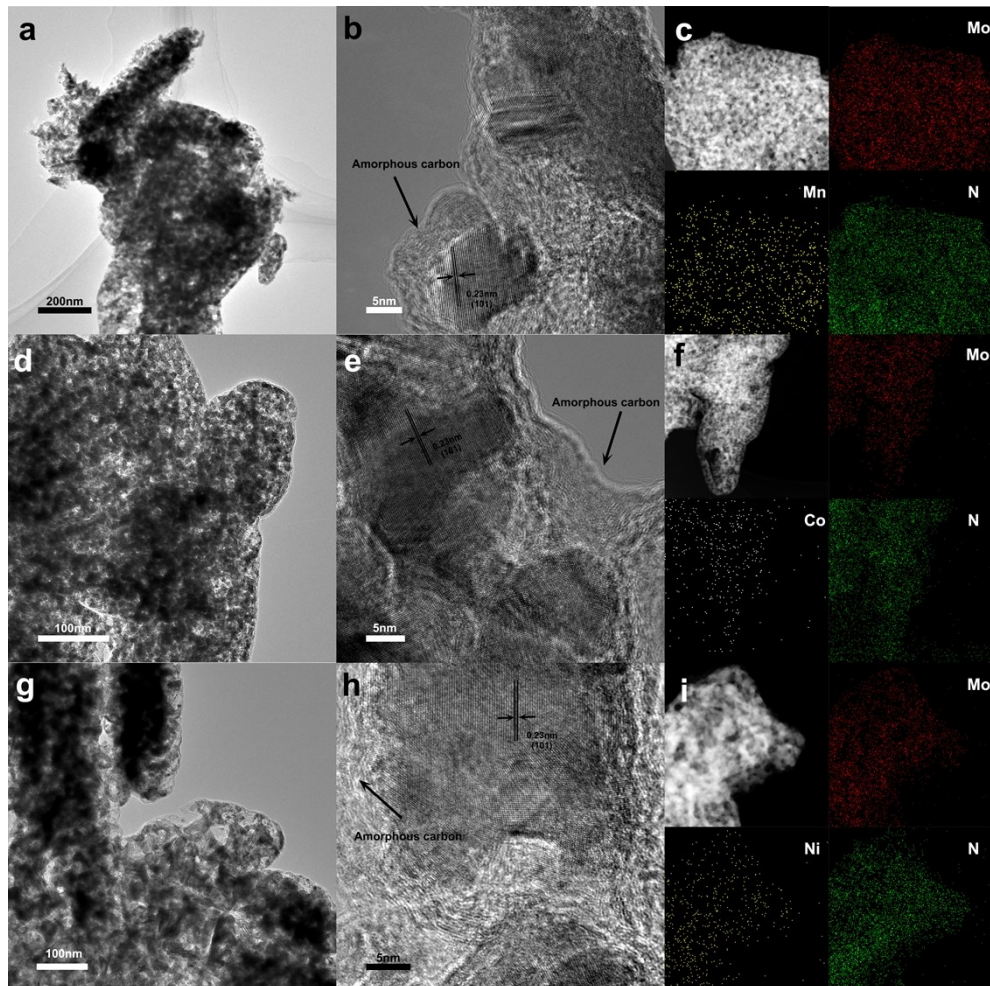


Figure S7. Raman spectra of undoped Mo₂C and 0.5%Fe-Mo₂C@NCF.

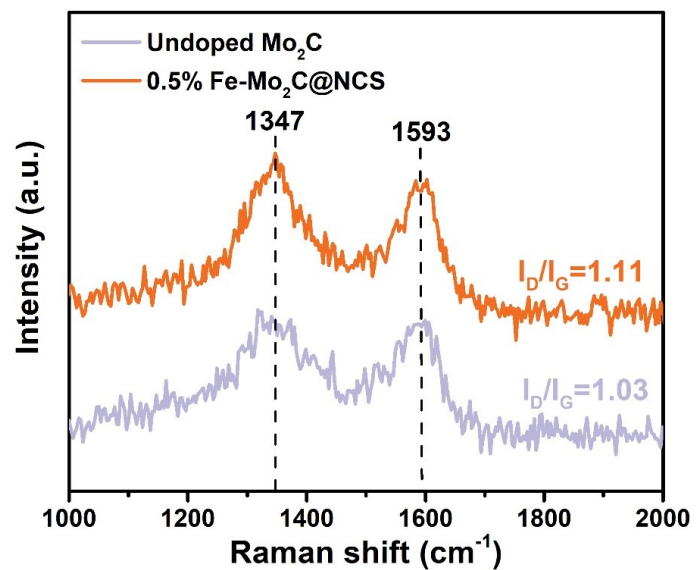


Figure S8. Summary of overpotential to reach 10 mA cm^{-2} (η_{10}) and overpotential to reach -100 mA cm^{-2} (η_{100}), the Tafel slopes and C_{dl} of (I): 0.2%Fe-Mo₂C@NCF, (II): 0.5%Fe-Mo₂C@NCF, (III): 1%Fe-Mo₂C@NCF, (IV): undoped Mo₂C in 1.0 M KOH (a), 1.0 M PBS (b) and 0.5 M H₂SO₄ (c).

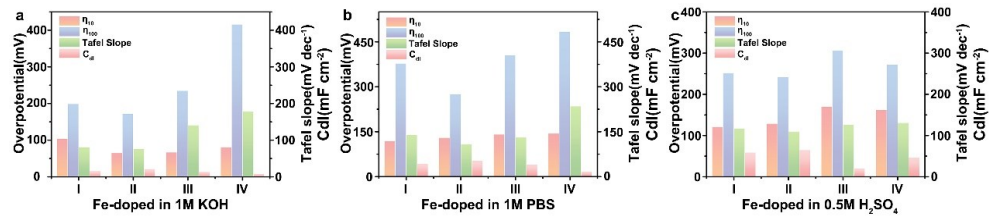


Figure S9. Cyclic voltammograms of 0.2%Fe–Mo₂C@NCF (I), 0.5%Fe–Mo₂C@NCF (II), 1%Fe–Mo₂C@NCF (III), undoped Mo₂C (IV) with various scan rates (from 10 to 100 mV/s) in 1.0 M KOH.

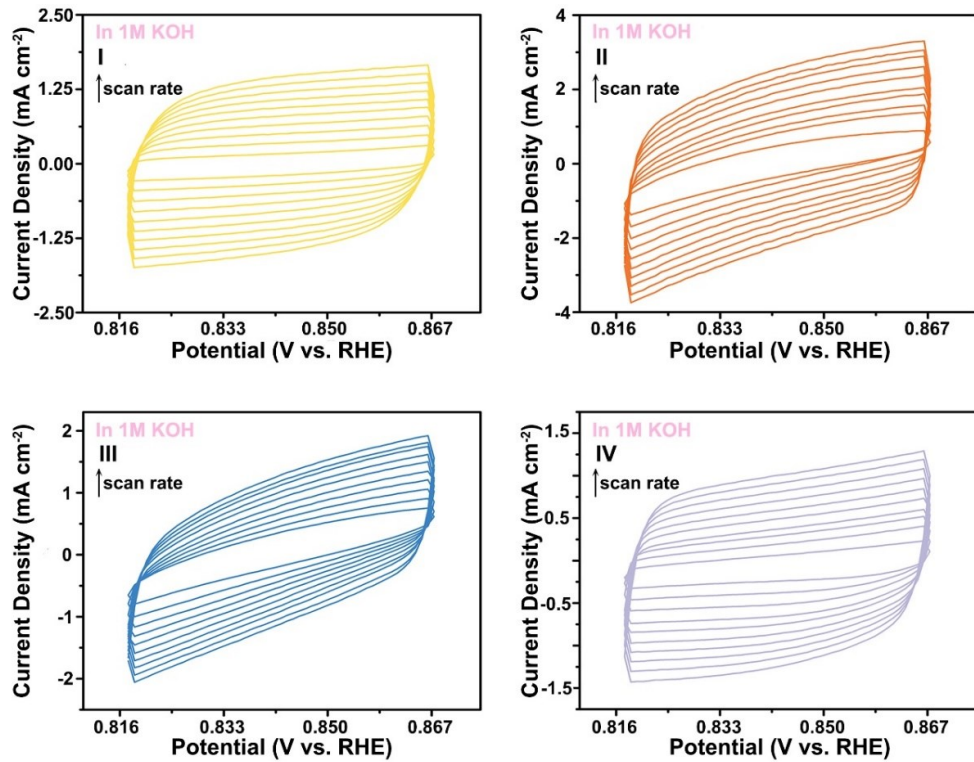


Figure S10. The iR-corrected LSV curves (a, b, c) and the Tafel slopes (d, e, f) of xMn-Mo₂C @NCF ($x = 0.2\%$ (I), 0.5% (II) and 1% (IV), respectively), undoped Mo₂C(IV). Comparison of the HER overpotentials for Mn-doped catalysts required to reach $j = 10/100 \text{ mA cm}^{-2}$ and the tafel slope in $0.5 \text{ M H}_2\text{SO}_4$ (g), 1.0 M PBS (h), 1.0 M KOH (i).

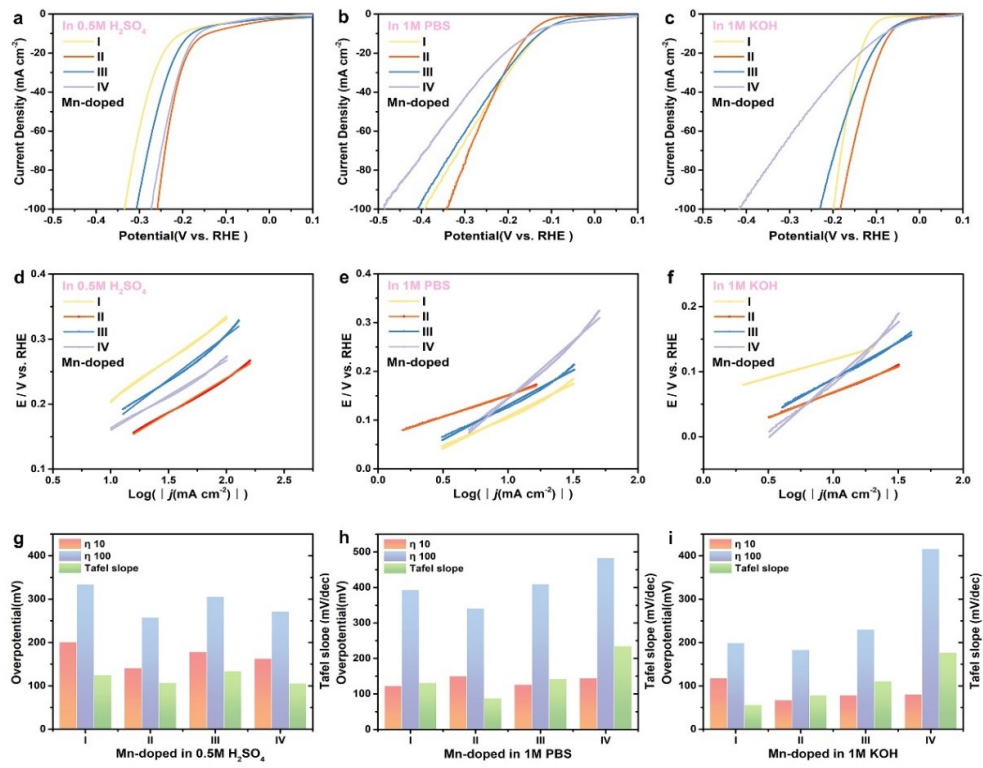


Figure S11. The iR-corrected LSV curves (a, b, c) and the Tafel slopes (d, e, f) of xCo-Mo₂C @NCF ($x = 0.2\%$ (I), 0.5% (II) and 1% (IV), respectively), undoped Mo₂C(IV). Comparison of the HER overpotentials for Co-doped catalysts required to reach $j = 10/100 \text{ mA cm}^{-2}$ and the tafel slope in 0.5 M H₂SO₄(g), 1.0 M PBS(h), 1.0 M KOH(i).

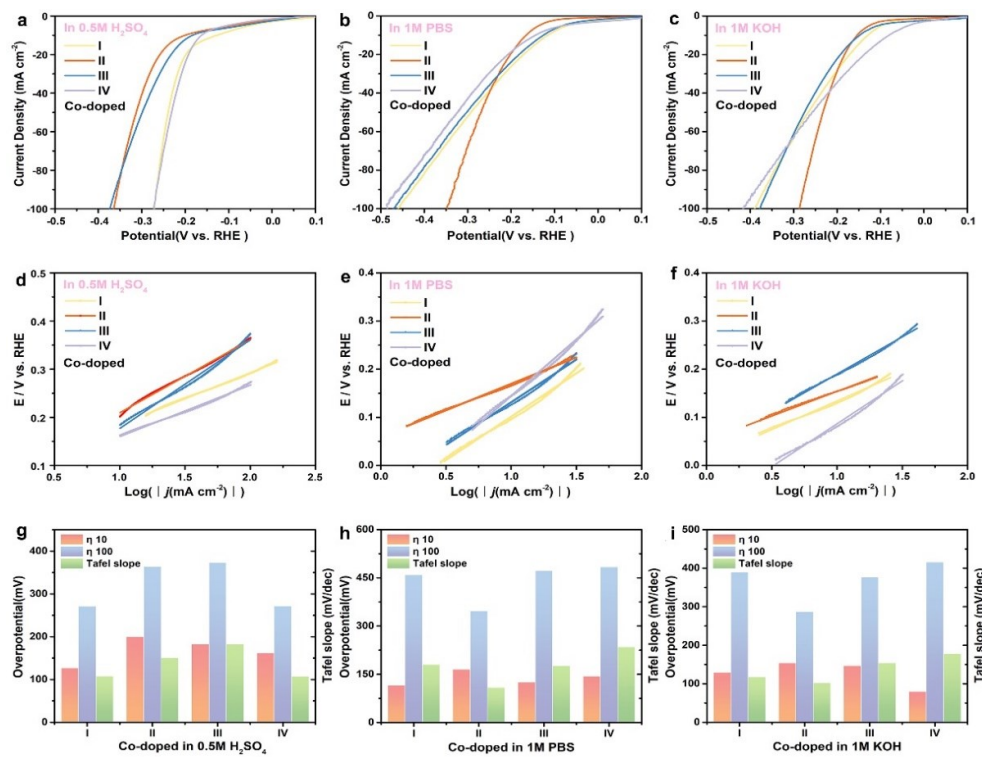


Figure S12. The iR-corrected LSV curves (a, b, c) and the Tafel slopes (d, e, f) of xNi-Mo₂C @NCF ($x = 0.2\%$ (I), 0.5% (II) and 1% (IV), respectively), undoped Mo₂C(IV). Comparison of the HER overpotentials for Ni-doped catalysts required to reach $j = 10/100 \text{ mA cm}^{-2}$ and the tafel slope in $0.5 \text{ M H}_2\text{SO}_4$ (g), 1.0 M PBS (h), 1.0 M KOH (i).

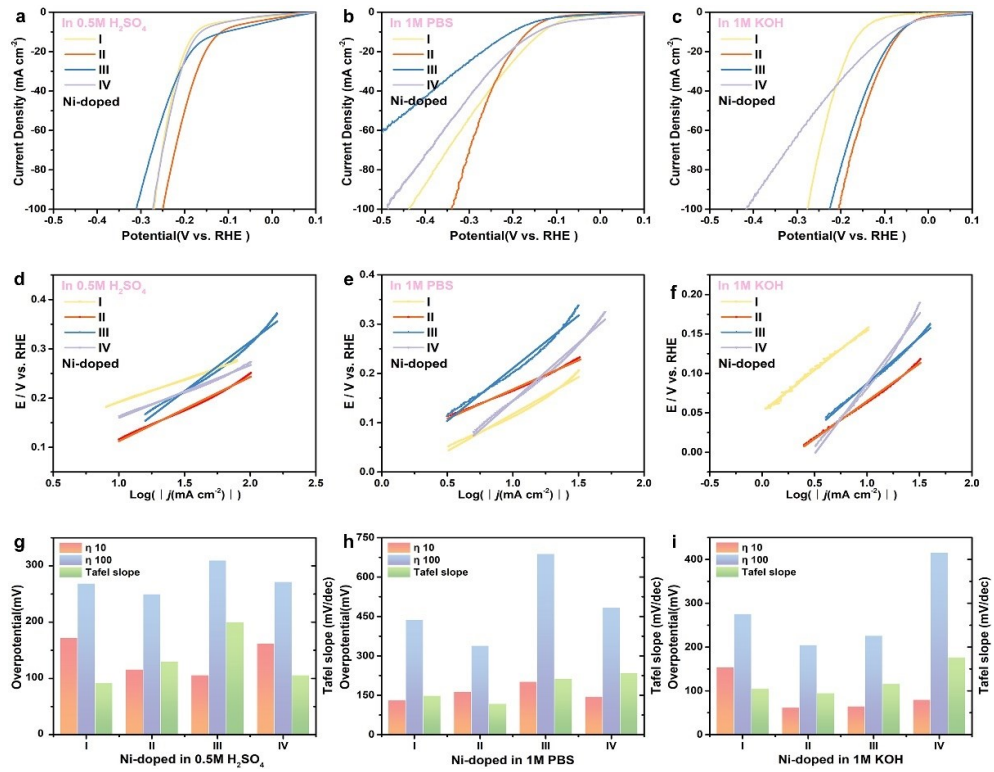


Table S4. Kinetic parameters for HER of 0.5%Fe-Mo₂C@NCF.

0.5%Fe-Mo ₂ C@NCF	η_{10} (mV)	η_{100} (mV)	Tafel slope (mV dec ⁻¹)	C_{dl} (mF cm ⁻²)
In 0.5 M H ₂ SO ₄	104	217	110	64.9
In 1.0 M PBS	121	267	209	53.6
In 1.0 M KOH	65	172	76	21.4

Table S5. Summary of the HER activity of undoped Mo₂C, 0.2%Fe-Mo₂C@NCF, 0.5%Fe-Mo₂C@NCF and 1%Fe-Mo₂C@NCF in 1.0 M KOH.

Catalysts (1.0 M KOH)	η_{10} (mV)	η_{100} (mV)	Tafel slope (mV dec ⁻¹)	C_{dl} (mF cm ⁻²)
undoped	81	416	178	8.1
0.2%Fe	104	199	80	15.9
0.5%Fe	65	172	76	21.4
1%Fe	67	235	141	13.8

Table S6. Summary of the HER activity of undoped Mo₂C, 0.2%Fe-Mo₂C@NCF, 0.5%Fe-Mo₂C@NCF and 1%Fe-Mo₂C@NCF in 1.0 M PBS.

Catalysts (1.0 M PBS)	η_{10} (mV)	η_{100} (mV)	Tafel slope (mV dec ⁻¹)	C_{dl} (mF cm ⁻²)
undoped	144	484	235	17.5
0.2%Fe	119	378	140	43.6
0.5%Fe	121	267	109	53.6
1%Fe	141	406	131	40.7

Table S7. Summary of the HER activity of undoped Mo₂C, 0.2%Fe-Mo₂C@NCF, 0.5%Fe-Mo₂C@NCF and 1%Fe-Mo₂C@NCF in 0.5 M H₂SO₄.

Catalysts (0.5 M H ₂ SO ₄)	η_{10} (mV)	η_{100} (mV)	Tafel slope (mV dec ⁻¹)	C_{dl} (mF cm ⁻²)
undoped	162	272	131	46.9
0.2%Fe	121	252	117	59.1
0.5%Fe	104	217	110	64.9
1%Fe	170	306	126	20.5

Table S8. Summary of the HER activity of Mn-Mo₂C@NCF, Co-Mo₂C@NCF and Ni-Mo₂C@NCF in 0.5 M H₂SO₄.

Catalysts (0.5M H ₂ SO ₄)	η_{10} (mV)	η_{100} (mV)	Tafel slope (mV dec ⁻¹)
0.2%Mn	201	334	125
0.5%Mn	141	258	107
1%Mn	178	306	134
0.2%Co	127	271	108
0.5%Co	200	364	151
1%Co	183	373	183
0.2%Ni	172	269	92
0.5%Ni	116	250	130
1%Ni	106	310	200

Table S9. Summary of the HER activity of Mn-Mo₂C@NCF, Co-Mo₂C@NCF and Ni-Mo₂C@NCF in 1.0 M PBS.

Catalysts (1.0 M PBS)	η_{10} (mV)	η_{100} (mV)	Tafel slope (mV dec ⁻¹)
0.2%Mn	123	393	132
0.5%Mn	150	341	88
1%Mn	126	410	142
0.2%Co	115	459	180
0.5%Co	165	347	109
1%Co	125	472	177
0.2%Ni	131	437	149
0.5%Ni	164	339	118
1%Ni	202	689	213

Table S10. Summary of the HER activity of Mn-Mo₂C@NCF, Co-Mo₂C@NCF and Ni-Mo₂C@NCF in 1.0 M KOH.

Catalysts (1.0 M KOH)	η_{10} (mV)	η_{100} (mV)	Tafel slope (mV dec ⁻¹)
0.2%Mn	118	199	56
0.5%Mn	67	183	78
1%Mn	78	230	111
0.2%Co	129	390	118
0.5%Co	154	287	102
1%Co	147	377	154
0.2%Ni	154	276	105
0.5%Ni	62	205	95

1%Ni	65	226	116
------	----	-----	-----

Table S11. Comparison of HER performance of 0.5%Fe-Mo₂C@NCF with other Mo-based HER electrocatalysts in 0.5 M H₂SO₄ solution.

Catalysts	Tafel Slope (mV/dec)	η_{10} (mV)	η_{100} (mV)	C_{dl} (mF/cm ⁻²)	Reference
Mo/Mo ₂ C-HNS-750	~68	89	/	~22	1
MoC _x nano-octahedrons	53	142	> 220	/	2
Mo ₂ C/C HCSs	75	153	~230	20.7	3
Co-Mo ₂ C-0.020	39	140	~210	~7.5	4
Mo ₂ C/NCNT-30	75	195	~350	/	5
Mo ₂ C@NPC	60.5	117	~175	28	6
Mo ₂ C-0.5% Fe@NCF	110	104	217	64.9	This work

Table S12. Comparison of HER performance of 0.5%Fe-Mo₂C@NCF with other Mo-based HER electrocatalysts in 1.0 M KOH solution.

Catalysts	Tafel Slope (mV/dec)	η_{10} (mV)	η_{100} (mV)	C_{dl} (mF/cm ⁻²)	Reference
Mo/Mo ₂ C-HNS-750	~63	79	~235	20.7	1
MoC _x nano-octahedrons	59	151	/	/	2
Co-Mo ₂ C-0.020	44	140	200	6.94	4
Mo ₂ C@NPC	73.5	121	~225	20.1	6
Mo ₂ C-0.5% Fe@NCF	76	65	172	21.4	This work

2. Theoretical Section

2.1 Computation details

All the density functional theory (DFT) calculations were performed via the Vienna Ab initio Simulation package (VASP),⁷⁻¹⁰ and the projector-augmented plane wave (PAW) pseudopotentials were used for the elements involved.¹¹ The generalized gradient approximation (GGA) of Perdew, Burke, and Ernzerhof (PBE) was used to treat the exchange-correlation between electrons.¹² The pristine β -Mo₂C (101) slab calculated in this study is shown in Figure 1 and the bottom 2 layers keep fixed during the calculation. A vacuum region of greater than 15 Å was added along the direction normal to the slab plane to avoid the interaction between periodic supercells. The electron wave function is expanded in plane waves and a cutoff energy of 550 eV is chosen. Gamma centered k-point meshed of (9, 9, 1) and (9, 9, 9) was adopted for the Brillouin zone (BZ) of the slabs and primitive cell. The convergence in the energy and force were set to be 10^{-4} eV and 0.02 eV/Å, respectively.

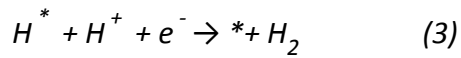
The free energies of H₂O(l) and H₂(g) were used as references when calculating the free energies of reaction intermediates. The adsorption energy for reaction intermediate is calculated as follows:¹³

$$\Delta G = \Delta E_{Total} + \Delta E_{ZEP} - T\Delta S + \Delta G_s - 0.0592PH - eU \quad (1)$$

where ΔE_{Total} is the calculated adsorption total energy by DFT, ΔE_{ZPE} is zero-point energy, ΔS is entropy, and ΔG_s is solvation energy.

For hydrogen evolution reaction (HER), the elementary steps are:





where * denotes a possible reaction site. The calculated HER electrochemical potential can be obtained as follows:

$$U_L = \text{Min}_i [-\Delta G_i]/ne \quad (4)$$

where n is the number of electrons transferred for each electrochemical step, and e is the elementary charge. Here, the n is set to 1 for the one-electron transfer step. The meaning of the right-hand side of the above equation is to select the smallest $[-\Delta G_i]$ among the HER elementary steps.

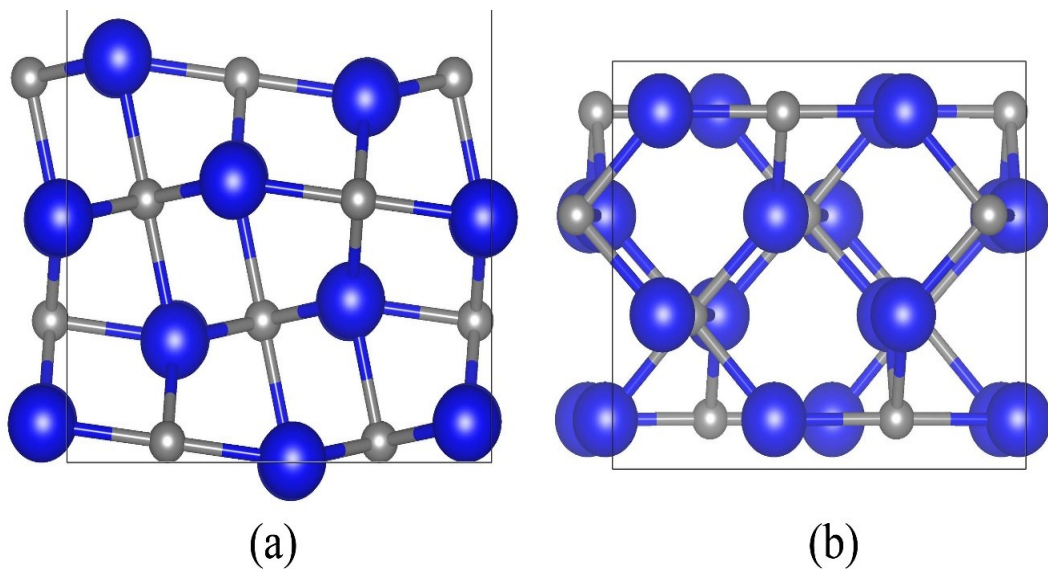


Figure S13. (a) side view and (b) top view of Mo_2C (101) slab, (blue ball, Mo; grey ball, C).

2.2 Theoretical models

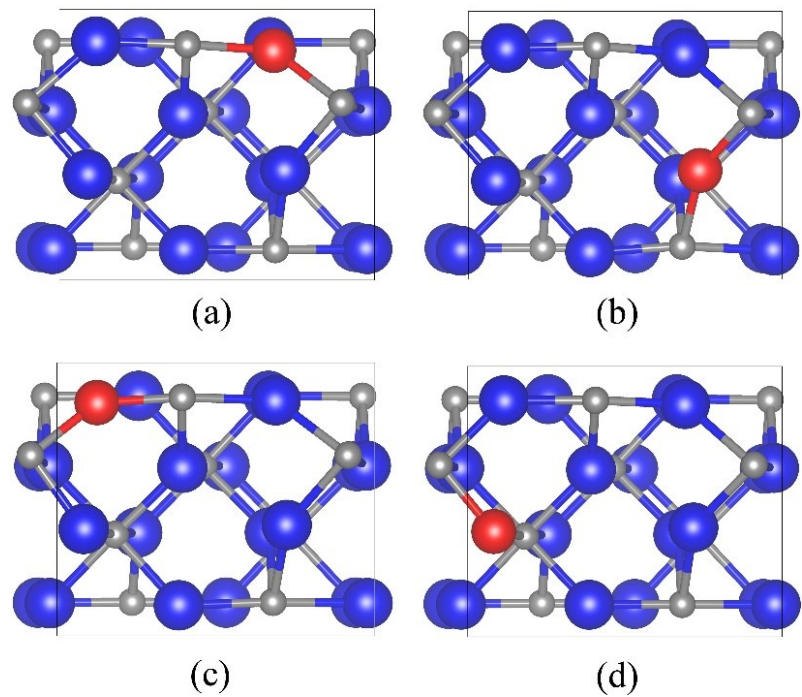


Figure S14. Atomic structures of 0.5%Fe-Mo₂C@NCF, (blue ball, Mo; grey ball, C; red ball, Fe).

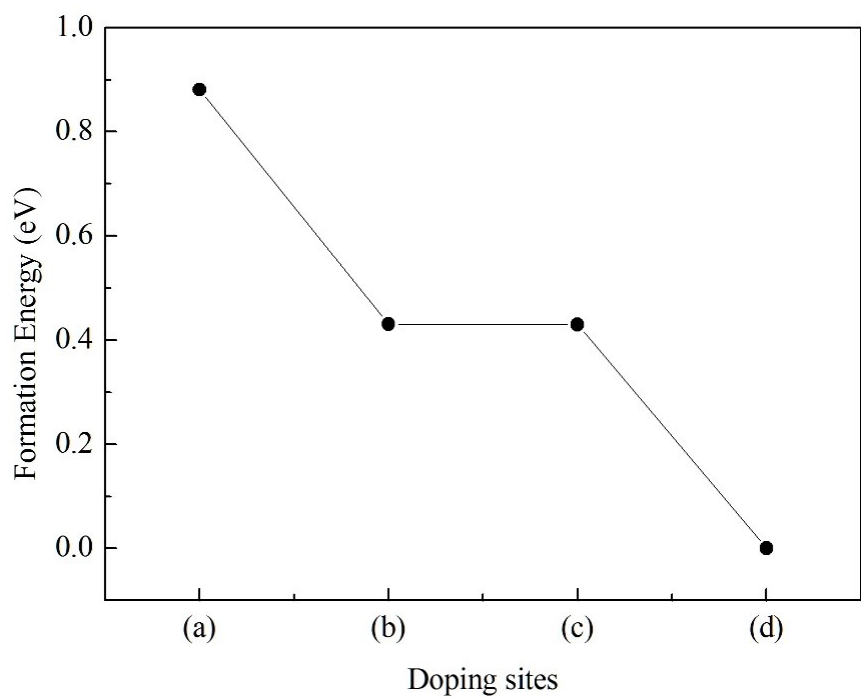


Figure S15. Formation energies of the structures with one Fe doping in different sites correspond to **Figures S14**, (the lowest formation energy among four structures is set to 0).

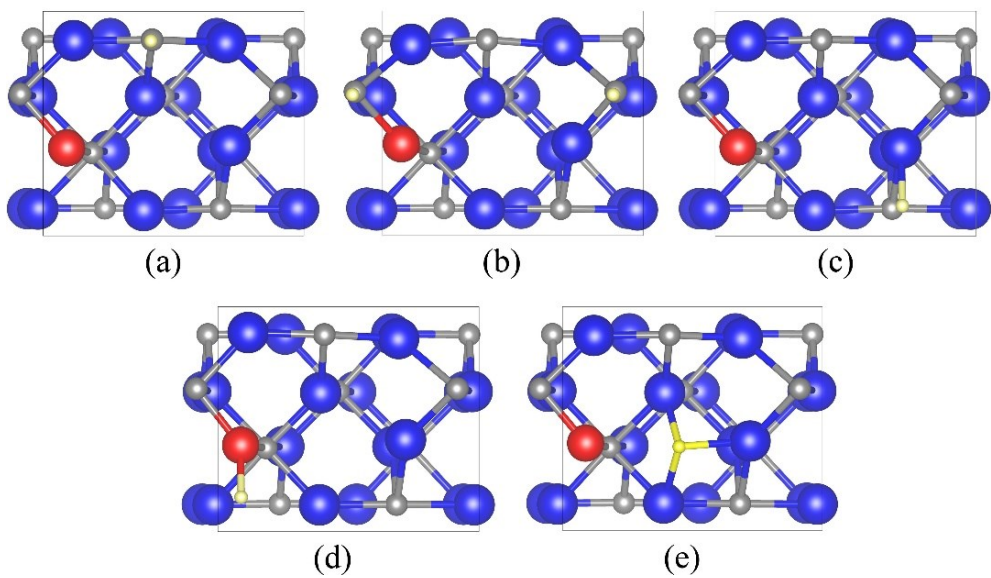


Figure S16. H adsorbed on different sites of pristine $\text{Mo}_2\text{C}:1\text{Fe}$ (101) surface, (blue ball, Mo; grey ball, C; red ball, Fe; yellow ball, H).

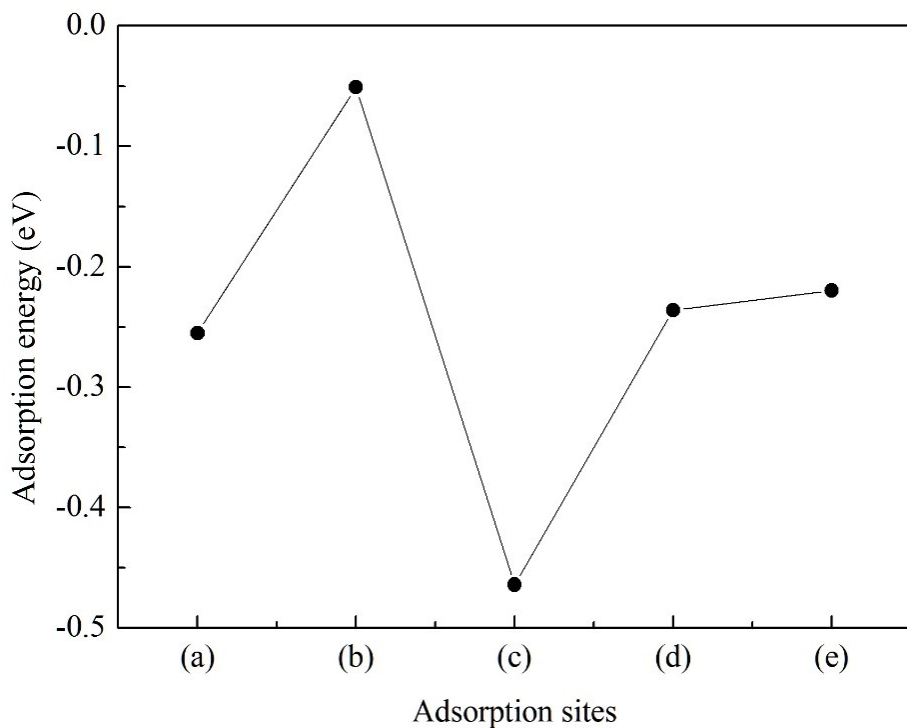


Figure S17. H^* adsorption energies of the adsorption sites correspond to **Figure S16**.

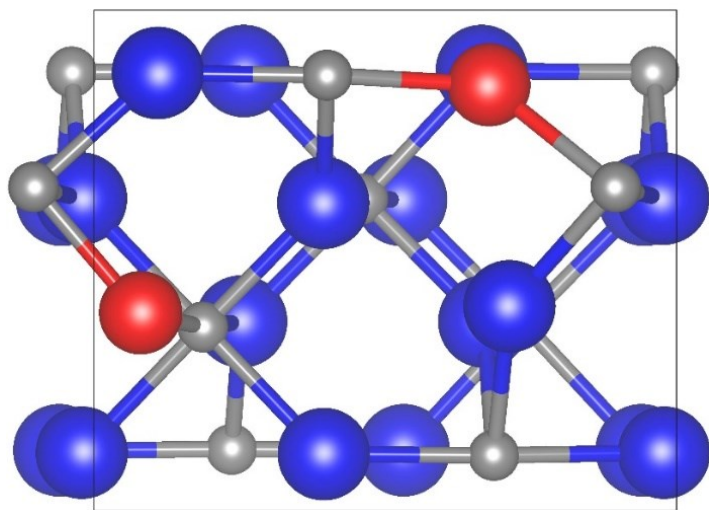


Figure S18. Atomic structures of 1%Fe-Mo₂C@NCF (blue ball, Mo; grey ball, C; red ball, Fe).

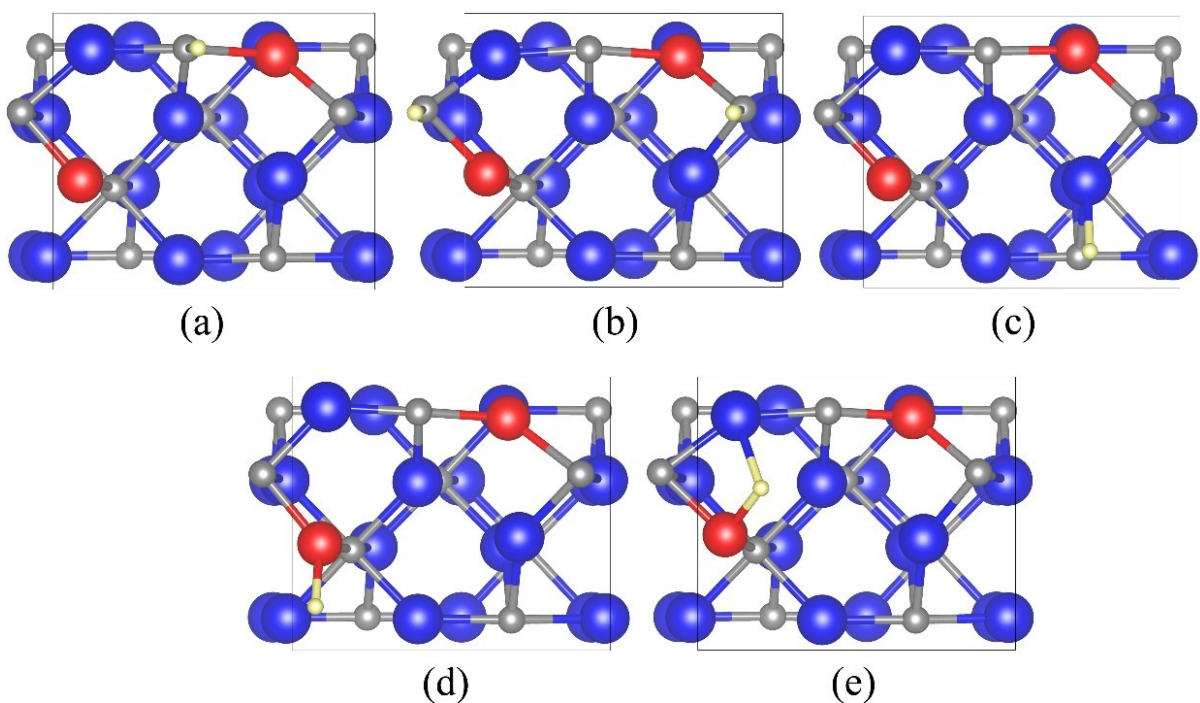


Figure S19. H adsorbed on different sites of 1%Fe-Mo₂C@NCF (101) surface, (blue ball, Mo; grey ball, C; red ball, Fe; yellow ball, H).

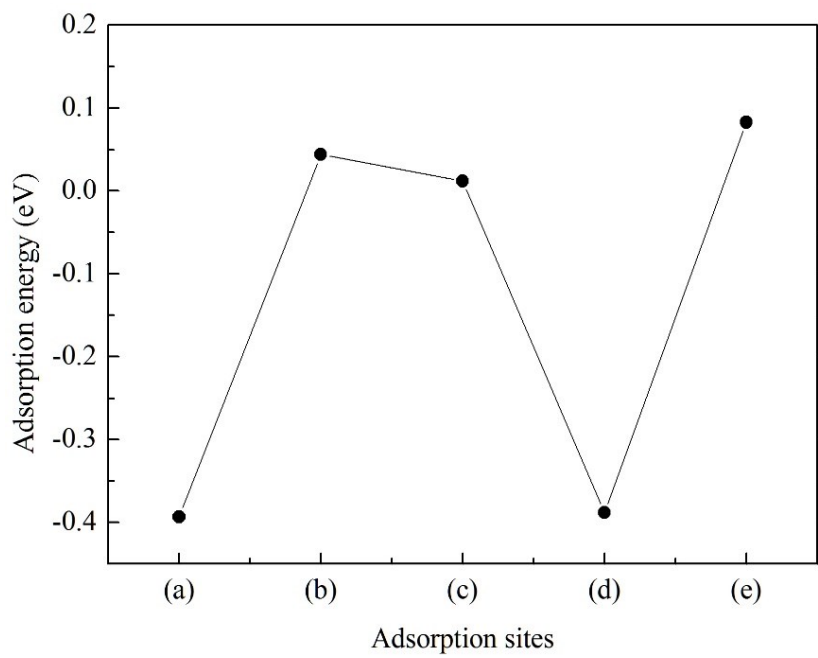


Figure S20. H^* adsorption energies of the adsorption sites correspond to **Figure S19**.

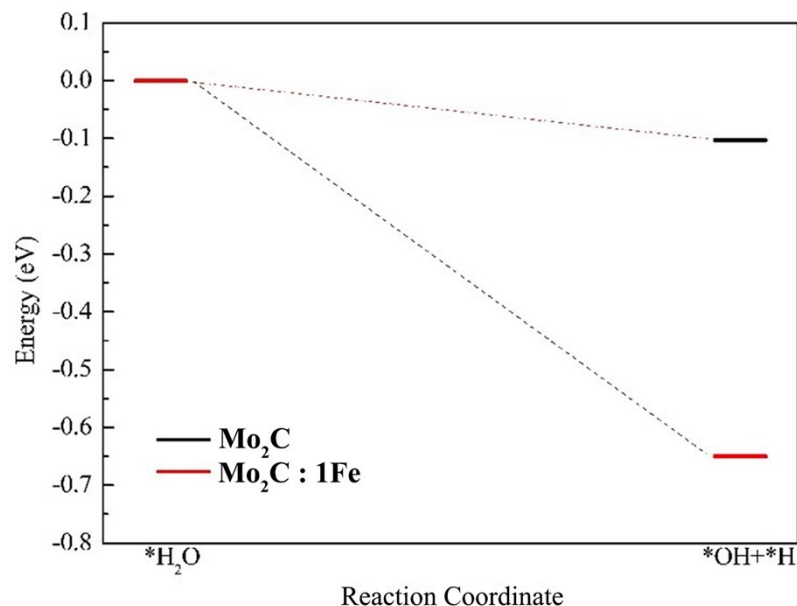


Figure S21. The Gibbs free energy diagram of water dissociation process on Mo_2C and $\text{Mo}_2\text{C}:1\text{Fe}$.

References

1. J. Xiong, J. Li, J. Shi, X. Zhang, N.-T. Suen, Z. Liu, Y. Huang, G. Xu, W. Cai, X. Lei, L. Feng, Z. Yang, L. Huang and H. Cheng, *ACS Energy Lett.*, 2018, 3, 341-348.
2. H. B. Wu, B. Y. Xia, L. Yu, X. Y. Yu and X. W. Lou, *Nat. Commun.*, 2015, 6, 6512.
3. Y. Yang, M. Luo, Y. Xing, S. Wang, W. Zhang, F. Lv, Y. Li, Y. Zhang, W. Wang and S. Guo, *Adv. Mater.*, 2018, 30, e1706085.
4. H. Lin, N. Liu, Z. Shi, Y. Guo, Y. Tang and Q. Gao, *Adv. Funct. Mater.*, 2016, 26, 5590-5598.
5. Y.-J. Song, J.-T. Ren, G. Yuan, Y. Yao, X. Liu and Z.-Y. Yuan, *J. Energy Chem.*, 2019, 38, 68-77.
6. K. Lan, L. Gong, M. Yang, X. Huang, P. Jiang, K. Wang, L. Ma and R. Li, *J. Colloid Interface Sci.*, 2019, 553, 148-155.
7. P. Hohenberg and W. Kohn, *Phys. Rev.*, 1964, 136, B864-B871.
8. G. Kresse and J. Hafner, *Phys. Rev. B*, Condensed matter, 1994, 49, 14251-14269.
9. G. Kresse and J. Furthmüller, *Phys. Rev. B*, 1996, 54, 11169-11186.
10. G. Kresse and J. Furthmüller, *Comp.mat.er.sci.*, 1996, 6, 0-50.
11. P. E. Blöchl, *Phys. Rev. B*, 1994, 50, 17953.
12. J. P. Perdew, K. Burke and M. Ernzerhof, *Phys. Rev. Lett.*, 1996, 77, 3865-3868.
13. J. K. Nørskov, J. Rossmeisl, A. Logadottir, L. Lindqvist, J. R. Kitchin, T. Bligaard and H. Jónsson, *J. Phys. Chem. B*, 2004, 108, 17886-17892.